E-MRS Spring Meeting 2011, Symposium S: Organic Photovoltaics: Science and Technology

Stable organic solar cells with Mg:Ag contacts

M. Rusu[*], F. Kraffert, S. Wiesner, W. Schindler, K. Fostiropoulos, M. Ch. Lux-Steiner

Institut für Heterogene Materialsysteme, Helmholtz-Zentrum Berlin für Materialien und Energie GmbH, Lise-Meitner Campus, Hahn-Meitner-Platz 1, 14109 Berlin, Germany

Abstract

Stable and efficient organic solar cells with Mg (20 at. %) : Ag alloy cathodes and bulk-heterojunction absorber layers from metal (e.g., Cu, Zn)-phthalocyanine and C_{60} small molecules are demonstrated. Device efficiencies of 4.0% under an illumination of 100 mW/cm^2 at 25°C were achieved as a result of the fine adjustment of the cathode work function as well as of the absorber design. By combining low and high work function materials, the work function in both Mg/Ag bilayer and Mg:Ag alloy layer cathodes was adjusted for optimum photovoltaic parameters. The electric and photovoltaic properties of the devices are discussed with respect to the cathode layer structure. The formation of the absorber/cathode interface was investigated by x-ray photoelectron spectroscopy measurements (XPS). The work function of the absorber and cathode layers were determined from the XPS high binding energy cutoff (HBEC) spectra. For optimized devices, the work function of the cathode at the side adjacent to the absorber layer equals 4.0…4.1 eV. While devices with Mg/Ag *bilayer* contacts exhibit a 65% efficiency drop in the first month after the preparation, devices with Mg:Ag *alloy* contacts demonstrate stable photovoltaic parameters within the time of the study of ~ 1 year.

Selection and peer-review under responsibility of the European Material Research Society (E-MRS)

Keywords: Organic solar cells; Phthalocyanine; Fullerene C_{60}; Organic/inorganic interface; Mg-Ag electrodes; Degradation; Stability

---

Nomenclature

XPS	x-ray photoelectron spectroscopy
HBEC	high binding energy cutoff
Φ	work function
BLC	bi-layer cathode
ALC	alloy-layer cathode
FS	front surface
BS	back surface

---

[*] Corresponding author. *E-mail address:* rusu@helmholtz-berlin.de

1. Introduction

Remarkable progress in achieving high photovoltaic (PV) conversion efficiencies of organic solar cells (OSCs) is attributed to an optimized device architecture, which includes donor (D):acceptor (A) bulk heterojunction absorbers as well as optimized absorber/electrode interfaces. Particularly, the formation of an optimum absorber/cathode interface was stimulated by a previous study on the optimization of the cathode structure, i.e., in the investigation of bilayer cathode (BLC) configurations. Recently, effective charge selective Mg/Ag bilayer contacts for blend organic absorbers consisting of copper phthalocyanine donor and fullerene C_{60} acceptor have been demonstrated [1]. In addition, it has been shown that at the interface between the CuPc:C_{60} absorber and the Mg/Ag cathode a Mg:Ag alloy layer with an adjusted work function (Φ) and a composition close to that of Ag_3Mg forms. The activities towards the devolpment of Mg:Ag alloy-based electrodes are stimulated by the highly stable chemical and electronic properties of this alloy, resulting consequently also in a stable Φ [2]. In the alloy, the work function can be easily adjusted between $\Phi_{Mg} = 3.4$ eV and $\Phi_{Ag} = 4.7$ eV by simply changing the [Mg]:[Ag] ratio.

In this contribution, we report on the formation of effective charge selective Mg:Ag alloy-layer cathodes (ALC) for bulk heterojunction organic absorbers consisting of Me (e.g., Cu or Zn)-phthalocyanine (MePc) donor and fullerene (C_{60}) acceptor materials. Instead of only sequentially depositing Mg and Ag thin films as reported in the previous work, Mg and Ag are also co-deposited on top of the absorber layer to form an Mg:Ag alloy-layer cathode of an optimum composition. The chemical and electronic properties of the CuPc:C_{60}/Mg-Ag interface is investigated by x-ray photoelectron spectroscopy (XPS). The work function of the absorber and cathode layers are determined from the XPS high binding energy cutoff (HBEC) spectra. The respective findings are discussed in relation to the performance and electrical properties of corresponding MePc:C_{60}-based OSCs.

2. Experimental

Experiments were performed on glass/indium tin oxide (ITO)/3,4-polyethylenedioxythiophene:poly-styrene-sulfonate (PEDOT:PSS) (30%)/80-nm-MePc:C_{60}(1:1)/Mg-Ag solar cell devices. The MePc:C_{60} layers were deposited by physical vapour deposition (PVD) at a base pressure of 10^{-7} mbar. Mg and Ag layers were co-deposited to form Mg:Ag alloy-layer contacts. In order to find an optimum Mg:Ag composition for investigated solar cells, the nominal Mg concentration was varied between 0 and 50 at. %. Reference devices with sequentially deposited Mg/Ag bilayer contacts were prepared according to Ref. 1. The chemistry and electronics of the absorber/contact interface was investigated (i) on MePc:C_{60} subcontact (Sbc) region, as well as (ii) on the back surface (BS) of both Mg/Ag and Mg:Ag contacts. Respective samples were prepared by lifting-off the metallic contacts in an N_2-filled glovebox. Additionally, front surface (FS) measurements were performed (iii) on the Mg-Ag surface of the ALC/ and BLC/MePc:C_{60}/PEDOT/ITO/glass stacks and (iv) on "pure absorber" (Abs-Pure) areas. The samples were transferred to the XPS system by a high vacuum ($\approx 10^{-8}$ mbar) shuttle.

The XPS surface sensitive measurements were carried out under UHV conditions (base pressure $<10^{-10}$ mbar). The data were recorded using Mg K_α x-ray radiation (1253.6 eV, source Specs XR 50) and a Specs Phoibos 100 electron spectrometer. The electron spectrometer was calibrated according to Ref. 3 using XPS and Auger line positions of different metals (Cu $3p$, Au $4f_{7/2}$, Cu L_3MM, and Cu $2p_{3/2}$). Standard settings for the electron spectrometer pass energy were 10 eV for the HBEC spectra and 30 eV for the XPS overview spectra, respectively. The XPS overview spectra were measured at the maximum power of 250 W of the x-ray tube. A -5 V bias was applied to the sample during the XPS-HBEC measurements in order to distinguish between the analyzer and sample cutoffs. In addition, XPS high binding energy cutoffs were measured at a lower x-ray power of 10 W with the x-ray gun retracted by 37 mm from the regular measurement position in order to further reduce the photon flux and minimize the presence of stray electrons photoemitted from the Al bremsstrahlung filter window. The work function was determined by linearly fitting the high binding energy cutoffs of the spectra and extrapolating to zero. To account for the analyzer broadening of 0.2 eV, the obtained HBEC values at the intersection points were corrected by 0.1 eV.

The electrical parameters of the OSC devices with an area of 4.7 ɜ 0.1 mm^2 were determined from dark current-voltage (J-V) measurements. The PV parameters (power conversion efficiency (Eff), fill factor (FF), open circuit voltage (V_{oc}), short-circuit current density (J_{sc})) were determined from J-V measurements performed under an illumination of 100 mW/cm^2 (Ha-lamp) at 25°C.

The stability of devices was tested by performing J-V measurements on samples stored in the dark in an N_2-filled glovebox.

3. Results and discussion

3.1. Photovoltaic and electrical parameters

For a direct comparison of the influence of the Mg content in Mg:Ag *alloy* cathodes and Mg/Ag *bilayer* cathodes, first the influence of the Mg-layer thickness on the charge selectivity of the Mg/Ag bilayer cathode in reference
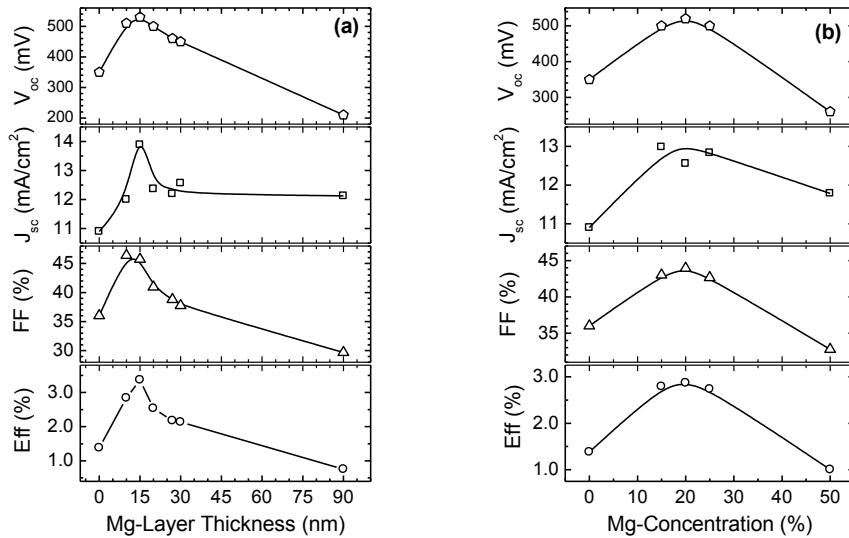

Fig. 1. PV parameters of ITO/PEDOT:PSS (30%)/80-nm-ZnPc:C_{60}(1:1) solar cells (a) with Mg/Ag bilayer cathodes of a fixed thickness of the Ag layer of 90 nm and a variable Mg-layer thickness and (b) with Mg:Ag alloy-layer cathodes with a variable Mg concentration. The data were recorded under an Ha-lamp illumination of 100 mW/cm² at 25°C.

ZnPc:C_{60}-based OSCs is studied by investigating the PV and electrical parameters of the bilayer cathode reference devices for Mg thicknesses ranging from 0 to 90 nm while keeping the Ag layer thickness constant at 90 nm. As depicted in Fig. 1(a), all PV parameters reach maximum values for a Mg-layer thicknesses of 15 nm. At the same time, the device series resistance (R_s) decreases dramatically, as can be seen in Fig. 2(a), while the parallel resistance (R_p) increases significantly. A further increase of the Mg thickness up to 90 nm results in a monotonic decrease of all the PV parameters. Simultaneously, R_s and R_p decrease to minimum values. Thus, an optimum Mg thickness of 15 nm is found for OSCs with ZnPc:C_{60} absorbers prepared by PVD.

Next, the influence of the Mg concentration in the 100 nm thick Mg:Ag *alloy* cathode layer on the device PV and electrical parameters is investigated as shown in Figs. 1(b) and 2(b), respectively. The device PV parameters reach a maximum at a Mg concentration of ≈20%. Thus the optimum cathode composition of ≈20%-Mg:80%-Ag is close to that of Ag_3Mg, which has been shown to be formed at the absorber/cathode interface of devices with Mg/Ag bilayer electrodes [1]. It is important to note that deviations from the optimum Mg concentration have a less critical influence on PV parameters of devices with *alloy* layer cathodes (ALCs) than in the case of deviations from optimum Mg-layer thickness in devices with *bilayer* cathodes (BLCs). This latter fact makes the application of Mg:Ag *alloy* cathodes technologically more attractive. Note that for the optimum cathode composition R_p values of 3-4 Ω×cm² are recorded, which are similar to those of BLC-devices. At the same time, R_s of the ALC-devices reach values of ≈0.8 Ω×cm², which are however much higher than those of the BLC-devices of ≈0.3 Ω×cm².
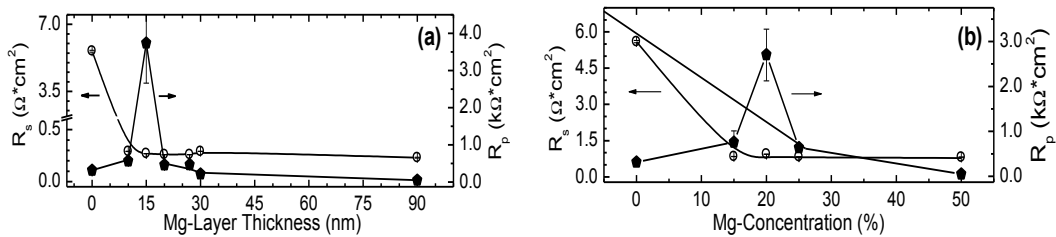

Fig. 2. The series (R_s) and parallel (R_p) resistances of the respective devices in Figs. 1(a) and 1(b).

It can clearly be seen that, in both optimisation experiments of the BLC- and ALC-structures, a good correlation between the behaviour of the devices V_{oc} and R_p exists. This strongly suggests that the adjustment of the cathode

structure/composition results in a simultaneous adjustment of the $\Phi_{cathode}$ thereby enabling an Ohmic contact to the n-type C_{60} and a blocking contact to the p-type MePc. The Ohmic nature of the 20%-Mg:80%-Ag alloy contacts to C_{60} was directly demonstrated on solar cell devices with an absorber structure of 50-nm-ZnPc:C_{60}/35-nm-C_{60}. With the latter absorber architecture 4.0%-effient solar cells with V_{oc}=540 mV, J_{sc}=15.0 mA/cm^2 and FF=48.9% were demonstrated. Efficiencies of 3.3% (for V_{oc}=540 mV, J_{sc}=12.9 mA/cm^2 and FF=48.0%) and 3.4% (for V_{oc}=530 mV, J_{sc}=13.9 mA/cm^2 and FF=45.7%) were achieved on solar cells with MePc:C_{60} absorbers and ALCs and BLCs, respectively. The higher efficiency of devices based on MePc:C_{60}/C_{60} structures is explained by higher short-circuit currents related to an improved spectral sensitivity (not shown) in the wavelength region between 400 and 600 nm due to the presence of the 35 nm thick C_{60} layer.

3.2. Absorber/cathode interface

To investigate the chemistry and electronics of the absorber/cathode interface, XPS measurements were performed on OSCs with both optimum 15 nm Mg/90 nm Ag bilayer and 20%-Mg:80%-Ag alloy cathodes. The XPS overview spectra revealed the elements present on each analyzed surface. A list of detected elements on each sample is presented in Table 1. No or negligible contamination of analyzed surfaces by carbon and/or oxygen was found. From ZnPc:C_{60} samples the emission peak C 1s (284 eV) is recorded. The O 1s emission peak (532 eV) is visible on Mg/Si reference and ALC20%-FS samples. In addition to the O 1s photoemission peak, the Auger electron peak from O *KLL* at 745 eV is visible, which is expected to originate from oxidized Mg^0 or adsorbed H$_2$O.

Table 1. The detected elements from XPS survey spectra together with work functions determined from HBEC spectra in Fig. 3 of the analyzed absorber and cathode surfaces. Ag/Si and Mg/Si samples are analyzed as references.

Sample	Detected elements	Φ_0 (eV)	Φ_1 (eV)	Φ_2 (eV)
Abs-Pure	N, C	4.32	-	-
Abs-Sbc	N, C, Mg, Ag	4.33	4.14	-
BLC15nm-FS	Ag	4.5	-	-
BLC15nm-BS	Mg, Ag	4.06	-	-
ALC20%-2nm	Mg, Ag, C	4.02	-	-
ALC20%-FS	Mg, Ag, O	4.08	3.56	4.42
ALC20%-BS	Mg, Ag	4.14	-	-
Ag/Si	Ag	4.50	-	-
Mg/Si	Mg, O	3.70	4.41	-

HBEC spectra in Fig. 3(a) reveal the work function of the pure absorber of 4.3Ⴠ0.1 eV as well as two work functions of the absorber surface left after the lift-off process. One of the work functions is similar to that of the pure absorber, while the second value of about 4.1 eV is attributed to some traces from lifted Mg-Ag contacts. In agreement with this assumption, values between 4.02 and 4.14 eV are recorded for the Mg:Ag alloy and the Mg/Ag bilayer on the back surface of both BLC- and ALC-samples as well as on the front surface of the organic absorber covered by a 2 nm thick layer of 20%-Mg:80%-Ag in Fig. 3(b). These results further support our model on the formation of an Mg:Ag alloy layer for sequentially deposited Mg and Ag films in the bilayer cathode [1]. In the HBEC top side spectra of the Mg:Ag-alloy layer in Fig. 3(c) three work functions can be derived: Φ_0=4.08 eV, Φ_1=3.56 eV and Φ_2=4.42 eV. The first value of 4.08 eV can be attributed to the work function of the 20%-Mg:80%-Ag alloy layer. The second value of 3.56 eV can be assigned to pure Mg indicating that the surface of the Mg:Ag cathode is covered by few monolayers of pure Mg. The presence of pure Mg on the surface of the Mg:Ag alloy layer is likely related to the difference in boiling points of Ag ($T_{Ag-boiling}$ =2435 K) and Mg ($T_{Mg-boiling}$ =1363 K): Due to the much lower boiling point of Mg, Mg vapors will be condensed last after the deposition process is finished (shutter closed) resulting in a Mg enriched front surface. The last value of 4.42 eV is similar to that of a MgO single crystal with (111) orientation [4] suggesting that MgO is formed on the front side. This finding is in good agreement with the observation of the O *KLL* Auger electron peak in the XPS overview spectra indicating the presence of oxidized Mg^0.
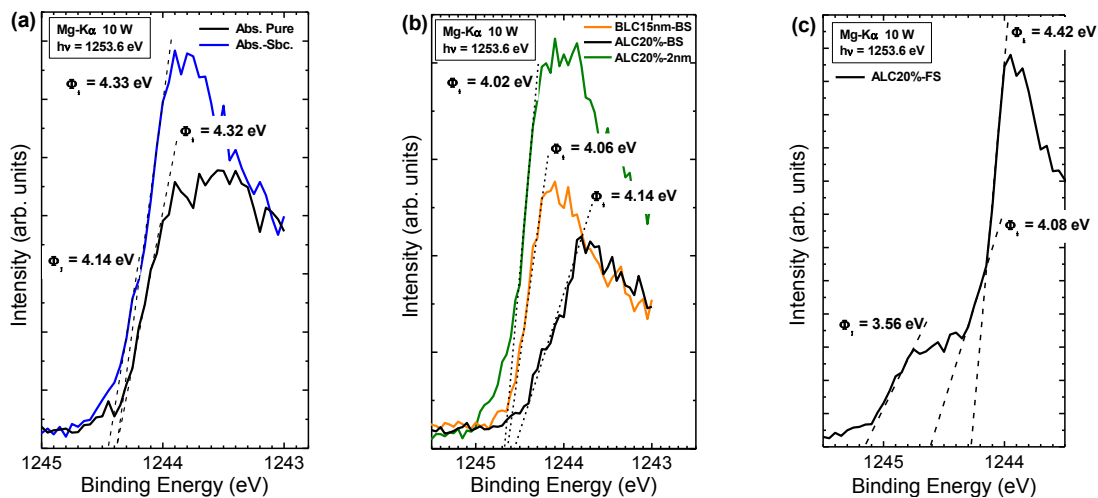
Fig. 3. HBEC spectra (a) of pure and subcontact surfaces of the ZnPc:C_{60} absorber, (b) of back surfaces of the Mg/Ag bilayer and Mg:Ag alloy layer cathodes in comparison to the front-side measurement on ZnPc:C_{60} absorber covered by a 2 nm thick 20%-Mg:80%-Ag layer and (c) of the front side of 100 nm thick alloy layer cathode (20%-Mg:80%-Ag).

3.3. Device stability

The stability of the devices stored in the dark in an N_2-filled glovebox is investigated as a function of the cathode structure. As it is seen from Fig. 4 devices with Mg/Ag bilayer contacts show a fast degradation exhibiting a 65% efficiency drop in the first month after the preparation. In contrast, devices with Mg:Ag alloy contact layers demonstrate stable photovoltaic parameters exhibiting negligible degradation within the investigated period of time of about one year. The microscopic origin of this clearly different stability of the BLC- and ALC-samples is likely related to (i) diffusion and (ii) oxidation processes associated particularly to Mg. The efficiency behavior of BLC-devices could be explained by dynamic processes of the Mg/Ag alloy layer formation via interdiffusion at the Mg-Ag bilayer system. Moreover, it has been demonstrated for BLCs that the excess Mg at the absorber/cathode interface diffuses into absorber [1]. This process could create over time shunting pathways, thus lowering the devices' R_p and consequently their V_{oc}-s. Furthermore, another fraction of the pure Mg in BLC devices may be oxidized resulting in changes of the cathode work function and thus in deviations from the optimum value. The good stability of the ALC-devices clearly suggests a higher stability of the co-deposited Mg:Ag alloy contacts indicating that the previously discussed diffusion and oxidation processes are minor and therefore do not lead to important changes in the composition/work function of the alloy cathode, in strong contrast to the bilayer structure.
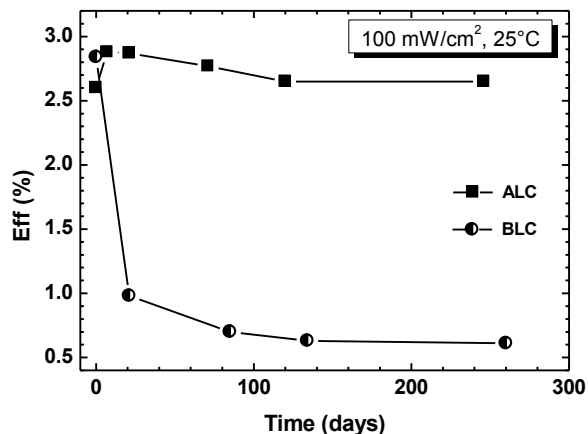

Fig. 4. Time dependence of the efficiency of ITO/PEDOT:PSS (30%)/80-nm-ZnPc:C_{60}(1:1) solar cell devices with 15-nm-Mg/90-nm-Ag bilayer cathodes (BLC) as well as of the devices with 25%-Mg:75%-Ag alloy layer cathodes (ALC). The data were recorded under an Ha-lamp illumination of 100 mW/cm^2 at 25°C.

4. Conclusions

In summary, the fine adjustment of the cathode work function for an Ohmic contact to the n-type C_{60} and a blocking contact to the p-type MePc could be achieved not only by the adjustment of the Mg thickness in the Mg/Ag bilayer architecture but also by the adjustment of the Mg concentration in the Mg:Ag alloy layer contact. The optimum cathode alloy composition of ≈20%-Mg:80%-Ag is close to that of Ag_3Mg, which has been previously shown to form at the absorber/cathode interface of devices with Mg/Ag bilayer electrodes [1]. The latter composition results in an optimum cathode work function for MePc/C_{60}-based OSCs that ranges between 4.0 and 4.1 eV. The Mg:Ag alloy cathodes with the optimum work function ensure at the MePc:C_{60}-absorber/cathode interface a simultaneous formation of (i) an Ohmic contact to the acceptor material (C_{60}) and (ii) a blocking contact to the donor material (MePc). Additionally, the Ohmic nature of the 20%-Mg:80%-Ag contacts to C_{60} was directly demonstrated on solar cell devices with an absorber structure of 50-nm-ZnPc:C_{60}/35-nm-C_{60}. With the latter absorber architecture a 4.0%-effcent solar cell has been shown. While the devices with Mg/Ag bilayer contacts show a fast degradation, the solar cells with Mg:Ag alloy-layer contacts show a good long-term stability.

Acknowledgements

References

[1] Rusu M, Wiesner S, Lauermann I, Fischer ChH, Fostiropoulos K, Audinot JN, Fleming Y, Lux-Steiner MCh. Formation of charge-selective Mg-Ag electrodes to CuPc:C_{60} blend layers. *Appl Phys Lett* 2010;**97**:073504/1-3.
[2] Miyagawa M, Koike R, Takahashi M, Bessho H, Hibino S, Tsuchiya I, Harano M, Endo M, and Taniguchi Y. Low work function MgAg-coated poly(ethylene terephthalate) films for organic light-emitting device fabrication with lamination process. *Jpn J Appl Phys* 2007;**46**:7483-7486.
[3] Briggs D, Seah MP. *Practical Surface Analysis*-, Auger and X-Ray Photoelectron Spectroscopy Vol. 1. New York. Wiley, 1990.
[4] Lim JY, Oh JS, Ko BD, Cho JW, Kang SO, Cho G, Uhm HS, Choi EH. Work function of MgO single crystals from ion-induces secondary electron emission coefficient. *J Appl Phys* 2003;**94**:764-769.